Bulletin of Environmental Contamination and Toxicology (2022) 109:865–871
https://doi.org/10.1007/s00128-022-03573-9

Application of SS-CS-HR-AAS measurements for the detection of Ag nanoparticles in marine invertebrates

Anna Maria Orani[1] · Emilia Vassileva[1] · Olivier P. Thomas[2]

Received: 31 January 2022 / Accepted: 23 June 2022 / Published online: 31 July 2022

Abstract

The present study describes the development of a fit-for-purpose analytical procedure for the detection of Ag NPs in different marine organisms by Solid Sampling Continuous Source High Resolution Atomic Absorption Spectrometry (SS-CS-HR-AAS). The detection is based on the observation of the Ag absorption peak and its atomization delay t_{ad} which is different for ionic Ag and Ag NPs. The temperature program was optimized in order to achieve the maximum difference between the t ad (Δt_{ad}). The method was first developed using biota CRMs spiked with different Ag NPs standard solutions or Ag^{+} , at the same concentration. Then, laboratory exposure experiments were performed on mussels and marine sponges. The results showed that the developed methodology is suitable for the detection of Ag NPs for both groups of organisms, showing Δt_{ad} up to 3.1 s. The developed method is therefore a promising tool to assess the presence of AgNPs in marine invertebrates.

Keywords Silver nanoparticles · Solid Sampling Atomic Absorbtion Spectrometry · Marine environment · Marine sponges · Mussels

Introduction

Nanomaterials are defined as materials of size between 1 and 100 nm (Handy et al. 2008b). Ag nanoparticles (NPs) are found in numerous applications such as disinfectants of manufacturing areas (including those in contact with water) (Adamek et al. 2018), antibacterial uses in water treatment, fabric softener, clothing, soft toys, wound dressing, kitchen utensils and appliances, among others (Shaw and Handy 2011). An important application of Ag NPs is represented by their use in food packaging. Recent studies under different experimental conditions have shown that Ag is potentially transferred from packaging to food in the form of NPs(Echegoyen and Nerín 2013; von Goetz et al. 2013; Jokar and Rahman 2014; Artiaga et al. 2015; Ntim et al. 2015). The rapid development and application of nanoparticles has resulted in increased input of these materials into the environment, including into aquatic and marine ecosystems since. estuaries and coastal areas are considered to be theoretical endpoints of contaminants such as NPs (Magesky and Pelletier 2018). Their widespread use has raised concern about their potential toxicity for a variety of aquatic and terrestrial organisms, including algae, invertebrates, plants and fish (Marambio-Jones and Hoek 2010; Fabrega et al. 2011; Magesky and Pelletier 2018; Zhang et al. 2018; Batista et al. 2020). It has been proven that exposure to Ag NPs can have negative effects on fish and several marine invertebrates, affecting both growth and survivability (Handy et al. 2008a; Shaw and Handy 2011; Abbott Chalew et al. 2012; Gomes et al. 2013; McCarthy et al. 2013; Magesky et al. 2016). In this context, the need for fast and reliable screening and detection methods for Ag NPs in environmental matrices is becoming a priority. The most recent analytical development for the detection, quantification and characterization of metallic NPs is the use of inductively coupled plasma mass spectrometry operating in single particle mode (sp-ICPMS). This methodology is sometimes supported by the use of a field flow fractionation system (AF^4-ICP-MS), to first separate the NPs from the

✉ Emilia Vassileva
e.vasileva-veleva@iaea.org

[1] International Atomic Energy Agency, Marine Environment Laboratories, 4 Quai Antoine 1er, 98000 Monaco, Principality of Monaco

[2] National University of Ireland, | NUI Galway · School of Chemistry, University Road, H91 TK33, Galway, Ireland

remaining matrix prior to analysis (Loeschner et al. 2013; Lee et al. 2014; Navratilova et al. 2015; Peters et al. 2015; Gagné et al. 2012) reported the first application of atomic absorption spectrometry to discriminate between Ag NPs and ionic form of Ag. The main limitations of these techniques are the time consuming sample preparation and the optimization of multi-step procedures including partial digestion and selective separation of NPs prior to element-specific instrumental detection (Tiede et al. 2009; Blasco and Picó 2011; Silva et al. 2011). Additionally, transformation of Ag NPs can occur during the multi-step sample preparation, causing biased results (Silva et al. 2011). High Resolution Continuous Source Atomic Absorption Spectrometry (HR-CS-AAS) has recently proven to be a powerful analytical tool in the detection of metallic nanoparticles (Resano et al. 2010, 2016; Leopold et al. 2017; Gruszka et al. 2018, 2021). Studies involving the use of SS-CS-HR-AAS were recently published for various matrices such as different food samples (Feichtmeier et al. 2016) and spiked dried parsley (Feichtmeier and Leopold 2014). As no sample preparation is required, the use of direct methods has drastically reduced the analysis time, representing a suitable alternative for the fast screening of Ag NPs in environmental monitoring. Most of these works based the detection of Ag NPs (and/or the distinction from ionic form of Ag) on observation of the absorbance peak, specifically the time at which maximum absorbance is observed (Feichtmeier and Leopold 2014). In this context, the aim of the present work was (1) to develop a method for the detection of AgNPs in marine invertebrates using SS-HR-CS-AAS, and (2) to apply the developed methodology to marine mussels and, for the first time, to sponges, preliminary exposed to Ag^+ and different sizes of Ag NPs. The method proved to be very appropriate for fast screening of Ag NPs in environmental and seafood monitoring studies.

Materials and methods

MilliQ water with resistivity ≥ 18 MΩ was used throughout the entire experimental work to both dilute standard solutions and to rinse the injection system. The Ag nanoparticles dispersions (sizes 10, 20, 40 and 60 nm) in aqueous solution at concentration of 20 mg L^{-1} as well as the Ag ionic solution at 1000 mg L^{-1} were obtained from Sigma Aldrich. For optimization of temperature programs, the solutions were diluted to a final concentration of about 3 µg L^{-1} using MilliQ water. The Certified Reference Materials (CRM) SRM 2976 (mussels' tissue, purchased by NIST, USA) and DORM-3 (dogfish muscle, from NRCC, Canada) were used during the experiments and optimization of the temperature program. Ag detection was carried out using a High-Resolution Continuum Source Atomic Absorption Spectrometer (ContrAA 700, Analytic Jena, Germany). This instrument is equipped with a graphite furnace atomizer, a Xenon short-arc lamp (GLE, Berlin, Germany) operating in "hotspot" mode as the radiation source, a high-resolution double echelle monochromator (DEMON), and a linear CCD array detector with 588 pixels, 200 of which are used for monitoring the analytical signal and performing background corrections. The CS SS HR AAS instrument operates with a transversely heated graphite tube atomizer and an automated solid sampling accessory (SSA 600). The solid sampling device incorporates a microbalance with a declared precision of 0.001 mg. The samples and standards were introduced using solid sampling graphite platforms. Argon with a purity of 99.999% (Air liquid, France) was used as purge and protective gas. The most sensitive Ag line at 328.07 nm was used for silver detection and measurement. The peak was integrated in peak volume mode using 3 pixels around the core line. All background corrections were conducted using the IBC (Iterative Background Correction) model available in the instrument software.

Two exposure experiments on living organisms were carried out: one on mussels and one on sponge samples. Mussels (21 specimens of *Mytilus edulis*) were manually collected in Arcachon Bay (Atlantic southwest coast of France). Sponges (16 specimens of *Acanthella acuta*) were collected by scuba diving in the Bay of Villefranche-sur-Mer (French Mediterranean coast). All the organisms were transported to the lab and transferred alive into aquariums, where they were left for 15 days to acclimate under flowing seawater. Both sponges and mussels were fed twice per day during the acclimatation and the exposure experiments. The experiments for each of the investigated species (mussels and sponges) involved 4 different aquaria: an aquarium with control samples, an aquarium spiked with Ag^+ solution, and aquaria spiked with 10 and 60 nm Ag NPs solutions respectively. The 10 and 60 nm sizes were selected because they showed the biggest difference (one from another) during preliminary experiments involving liquid standards. Between 3 and 6 specimens of mussels or sponges were placed in closed circuit aquaria and included for each experiment. The spike concentration for each aquarium was set as 5 µg L^{-1}, and the exposure experiment was carried out as follows: each aquarium was spiked with the mentioned Ag^+ or Ag NPs concentration for 12 h, then the organisms were fed with phytoplankton, the seawater was replaced with a clean portion, and the 5 µg L^{-1} spike was renewed. This cycle was repeated twice per day, and the total time of exposure was set at 96 h. The organisms were then carefully rinsed with clean seawater and euthanized by deep freezing (-18 °C). Subsequently samples were freeze-dried, manually ground in a mortar, and analyzed by HR-CS-AAS. This

experimental set up guaranteed the exposure of sponges and mussels to a continuous concentration of the respective contaminant, correcting for possible decrease in bioavailability. Additionally, with this set up, we prevent possible Ag depletion as a consequence of accumulation by the phytoplankton used to feed the sponges. Following the concept previously proposed by Feichtmeier and Leopold (Feichtmeier and Leopold 2014) and Feichtmeier et al. (Feichtmeier et al. 2016), the main parameter considered in the interpretation of our results was the so called "atomization delay" (t_{ad}), i.e. the time at which the maximum absorbance is registered for each peak. In theory, Ag^+ and Ag NPs will show measurably different t_{ad}, which makes differentiation between these two silver forms possible. The difference was defined as:

$$\Delta t_{ad} = t_{ad}(Ag^+) - t_{ad}(AgNP)$$

(1) where $t_{ad}(Ag^+)$ and $t_{ad}(AgNP)$ are the atomization delays (in s) measured for samples containing Ag^+ and Ag NPs, respectively. The differences were expected to be visible in liquid standards but also in spiked samples, as the interaction between the analytes and the sample matrix should influence the atomization delay.

Results and discussion

First, the temperature program was developed and optimized using liquid standard solution containing Ag^+ and Ag NPs of different sizes. Then, some biota CRMs in which the Ag content was not detectable, were spiked with Ag^+ and Ag NPs in order to observe a possible matrix effect. This was a necessary step, as no CRM certified for Ag NPs is available on the market. The third and final step of the experimental setting involved the exposure of living organisms (mussels and sponges) to Ag NPs (10 and 60 nm) and to the Ag^+ solutions, followed by the respective analyses. The main objective during the optimization of temperature programs was to maximize the observed difference in t_{ad}, Δt_{ad}. The optimized temperature programs used in this study are presented in Table 1 S (supplementary material). As expected, the use of a matrix modifier influenced the results. Specifically, even a permanent modifier such as Ir (often used in GF AAS) had the negative result of reducing the Δt_{ad} through thermal stabilization of the analyte. The experiments were therefore conducted without the use of matrix modifiers and using graphite platforms not pre-treated with Ir coating. Another factor which appeared to improve the separation between the two t_{ad} was the atomization temperature. Specifically, the results showed that a better separation between the two peaks can be obtained when decreasing the atomization temperature. Figures 1 and 2 S (supplementary material) show the peaks obtained when analyzing the Ag^+ and Ag NPs solutions using 2000 °C and 1000 °C atomization temperatures, respectively. This trend was previously observed by (Feichtmeier et al. 2016), who demonstrated the positive effect reducing atomization temperature had on Δt_{ad} values. Feichtmeier et al. determined Δt_{ad} ranging from − 0.77 to 1.39s for a series of different matrices, while in the present study it was possible to obtain Δt_{ad} values up to -2.9 s. When working at 2000 °C atomization temperature, the change of the pyrolysis temperature did not significantly improve the differentiation between peaks. Therefore, an optimum pyrolysis temperature of 300 °C was selected. This observation was also in agreement with a previous study showing that pyrolysis temperature above 400 °C resulted in insignificant differences and generally lower Δt_{ad} for different biological matrices (Feichtmeier et al. 2016). Figure 2 S shows that the Δt_{ad} values were different for different Ag NPs size. Specifically, the lowest Δt_{ad} was obtained when analyzing solutions of 10 nm Ag NPs, while the highest Δt_{ad} was obtained when measuring Ag NPs of 60 nm. The t_{ad} repeatability, estimated as RSD on 6 replicates measurements of different liquid standards, was found to be between 2 and 3%. To check the possible interactions of Ag^+, Ag NPs with the biological matrix, some experiments were carried out on solid biota spiked with 20 µL of the solutions. The selected biota CRMs had Ag contents below the detection limit of the technique, meaning that the solid itself, when analyzed by SS-HR-CS-AAS, did not show any detectable Ag peak. These materials were therefore suitable to be spiked, and to mimic the behavior of the biological matrix during the analysis. The spike of either Ag^+ or Ag NP solution was performed just before the analysis and added directly on the graphite platform containing about 0.2 mg of solid sample. The results obtained for these two materials are shown in Fig. 1, and the numerical values are reported in Table 2 S (supplementary material). As expected, the behavior of the peak varied with respect to the analyzed matrix, meaning that the obtained Δt_{ad} for the SRM2976 were different from those measured for DORM-2. The behavior of Ag when placed with SRM2976 was much closer to that of the liquid standard. The only exception was the 10 nm mix, which when combined with SRM2976, gave a Δt_{ad} much lower than the value obtained for the liquid standard alone. On the other hand, the DORM-3 material mixed with solutions containing Ag NPs generally led to a much lower Δt_{ad} when compared to liquid standards. It was already shown that the t_{ad} can vary greatly depending on the studied matrix. Specifically that increasing protein content leads to increased atomization delays (Feichtmeier et al. 2016), which then leads to a more negative Δt_{ad}. Biotic tissues with high protein content (e.g., mussels) retain more Ag, causing higher atomization delays. In the case of DORM-3, the Δt_{ad} obtained

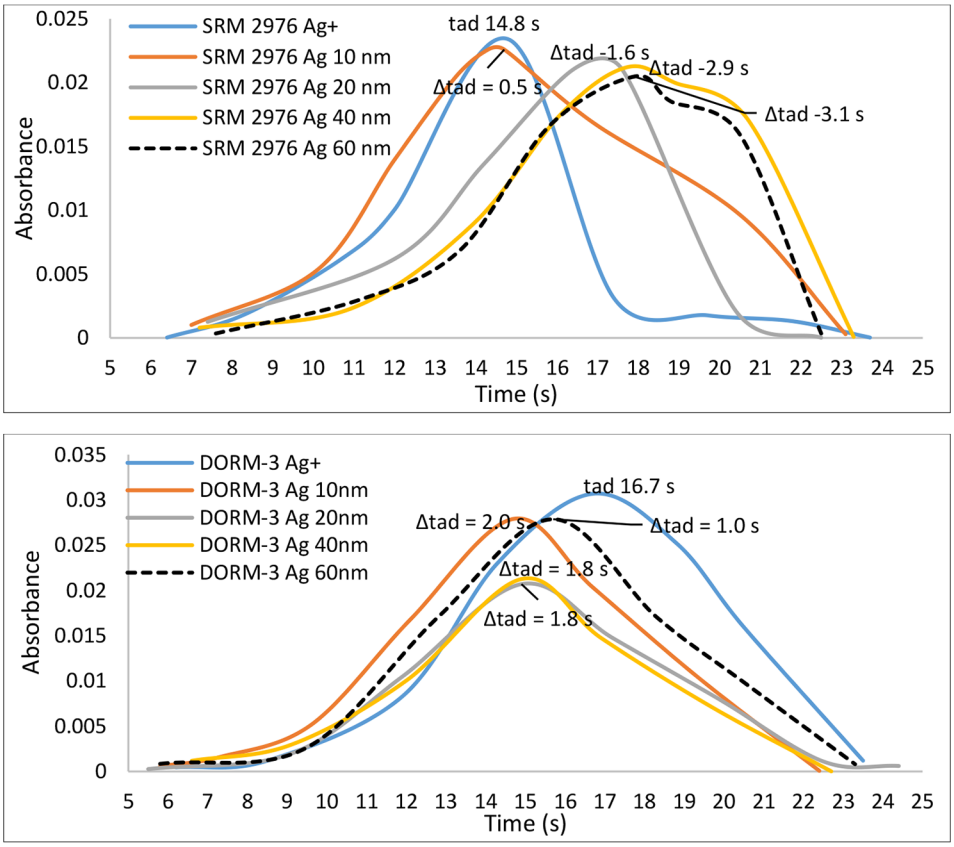

Fig. 1 Peaks obtained for the CRM materials SRM 2976 and DORM-3 spiked with 3 µg L^{-1} of either Ag^+ or Ag NPs of different sizes

for Ag NPs were in all cases positive, and the atomization delays were generally lower than for the mussel spiked with the same solution. One exception was the solid spiked with Ag^+, which presented much higher t_{ad} for DORM than for SRM2976. These data confirm that the interaction with different matrices, even matrices belonging to the same family (i.e., marine organisms) can affect the atomization delay of Ag. Even considering these differences, the method developed in the present study was always capable of distinguishing between Ag^+ and Ag NPs spiked samples, proving its robustness and flexibility for a rapid screening of these analytes. On the other hand, this type of experiment cannot guarantee that the homogeneity of the analyzed solid-liquid mixture is good enough for an accurate evaluation of the results. For this reason, spike experiments were then carried out on living organisms, during which the organism has the time to physically incorporate the different Ag forms.

The analyses on mussels exposed to different Ag species were performed directly on solid samples. The control mussels didn't show any detectable Ag peak when analyzed, meaning that the Ag content naturally present in the collected organisms was not detectable, when applying the developed method (Fig. 3 S, supplementary data). Peaks obtained for mussels spiked with Ag^+ and Ag NPs are shown in Fig. 2. The repeatability of the obtained t_{ad} was determined by measuring at least three times the same mussel specimen, and the calculated RSD was between 0.9 and 1.5%, regardless of the spiked sample considered. The robustness and reproducibility of the method were approved with regard to sufficient homogeneity of the micro samples, used for solid sampling and also regarding instrumental parameters such as individual solid sampling platforms, graphite tubes as well as measurements in different days. Replicate measurements with different solid sampling platforms and graphite tubes on several days still allows distinction of Ag NPs since the differences in t_{ad} were always significant. Limit of Detection (3s definition) was calculated via the monitoring of 10 blank replicates and the concentration of a calibration curve and was found to be 0.22 µgkg^{-1} using 0.1 mg control mussel's sample, proving the usefulness of the approach for LOD, for Ag NPs.

The reproducibility was also evaluated by measuring several specimens exposed to the same condition; this was also a way to evaluate the so-called intra-specie variability. The latter was again calculated as RSD and it was found to be in the range of 2–3% for each studied condition (Table 2 S,

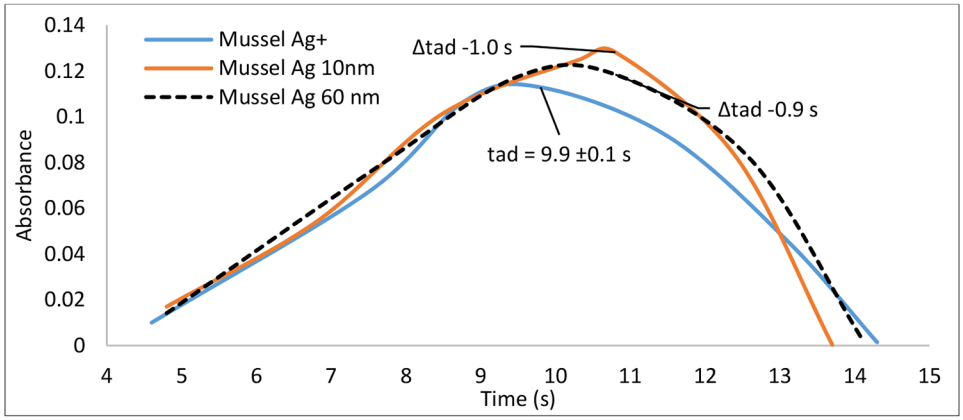

Fig. 2 Peaks obtained for mussel specimens (n = 5) spiked with3 µg L^{-1} Ag^+, Ag NPs 10 and 60 nm. The analyses were performed directly on the solid samples. The represented t_{ad} is calculated as average (n = 5 specimens) and presented with respective standard deviation. The Δt_{ad} were calculated using the respective average values of t_{ad}: the resulting combined uncertainty did not exceed 5%

supplementary material). In order to obtain comparable results through different conditions, the absorbances had to be in the same range, therefore the sample masses of the analyzed solid mussels were kept as close as possible and around 0.2 mg. Usually this amount of sample generated a total integrated absorbance of about 0.8. This adjustment was necessary because the total integrated absorbance might influence the peak shape, which in return could influence the t_{ad}. As a first conclusion, the application of the developed method is valid when a reference measurement of an individual specimen spiked with Ag^+ is available for comparison. This might represent the principal limitation of the present methodology and its application for real samples. Based on the measurement of a relative parameter (Δt_{ad}), the Ag^+ spike represents a type of one-point calibration for the provided qualitative method. The results obtained for mussels allow us to draw a very important conclusion: it is consistently possible to easily distinguish between specimens spiked with Ag^+ and Ag NPs. In these samples, the t_{ad} found for mussels spiked with Ag NPs are consistently higher than those found for Ag^+, resulting in negative values of Δt_{ad}. This result is consistent with previous findings, suggesting that Ag was efficiently taken up in the form of NPs, and did not undergo any transformation within the mussel tissue (Feichtmeier et al. 2016). The difference of behavior between Ag 10 and 60 nm was less clear than in the experiment carried out with liquid standard. This might be linked to the specific interaction with the biological matrix during the time at which mussels were exposed to Ag NPs. As expected, the observed behavior was rather different for the mussel CRM (SRM 2976) spiked with Ag^+ and different sizes of Ag NPs. This is easily explained when considering the possible low homogeneity and low interaction efficiency observed for the spiked solid powder compared to the living mussels. The Δt_{ad} calculated for the spiked CRM are closer to those obtained for liquid standards than to those obtained

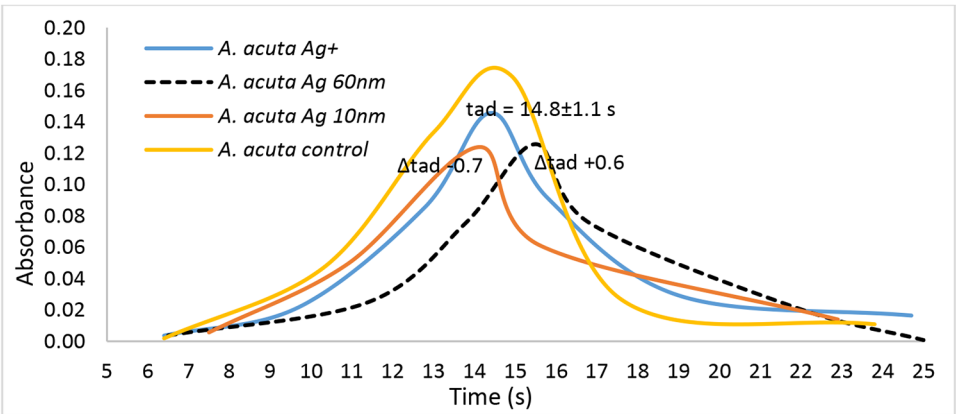

Fig. 3 Peaks obtained for sponge specimens (n = 5) exposed in the aquarium to 5 µg L^{-1} Ag^+, Ag NPs 10 and 60 nm. Due to the high Ag amount present in control samples, these analyses were performed on slurries, to reduce the Ag amount introduced in the furnace and to be able to highlight the differences in t_{ad}. The represented t_{ad} is calculated as average (n=5 specimens) and presented with respective standard deviation. The Δt_{ad} were calculated using the respective average values of t_{ad}: the resulting combined uncertainty didn't exceed 5%

for spiked mussel samples. Even though the Δt_{ad} obtained for spiked mussels and SRM 2976 were consistently negative, meaning that Ag NPs always showed higher t_{ad} than Ag^+, the numerical values obtained for the CRMs were generally different. Also, the difference between different Ag NPs sizes was more evident in the results obtained for the CRMs than in the spiked mussels. In addition to the low homogeneity, the insufficient mixing contact between the Ag solution and the solid sample could be responsible for this difference. In this context, the importance of real exposure experiments involving living organisms is particularly evident. The exposure experiment likely gives more accurate results, as it mimics a probable environmental exposure, during which the contaminant has time to be incorporated and possibly bio-transformed by the organism itself.

The major difference encountered when analyzing sponges was the high pre-existing Ag content in control samples. In order to provide reasonable and comparable graphs, it was necessary to analyze the sponge samples as slurries, in order to "dilute" the Ag content and allow for peak comparison. The slurries were prepared by adding a volume of about 10 mL of MilliQ water to about 0.1 g of the freeze-dried sponge samples. The sample mass and the added water were adjusted to obtain comparable absorbance during the experiment. A 20µL aliquot of slurry was manually injected and analyzed, originating peaks with a typical total absorbance of about 0.9. Repeatability was determined by measuring the same slurry solutions at least three times: the calculated RSD was generally below 1%, regardless of the spiked sample considered. The reproducibility (or intra-specie variability) was found to be ≤ 4% for each condition studied (Table 2 S). A graph summarizing the obtained results is presented in Fig. 3. Interestingly, the t_{ad} determined for control samples was very close to the one measured for Ag^+, meaning that the high Ag peak observed in control samples is likely ascribable to Ag in its ionic form rather than NPs. Therefore, the Ag peak observed in spiked samples was related to a natural mix of pre-existing ionic Ag and artificially added Ag NPs. Since in all cases it was possible to clearly distinguish the peaks of sponges spiked with either Ag + or Ag NPs, this proves the robustness of the developed method even when a mix of different Ag forms is present in real samples. The main difference in when comparing the sponge *A. acuta* to the mussels, is that even control samples of sponge show a very high silver content. This AG content was not quantified, as it was not the object of the present study but was clearly detectable with the optimized method. The sponge *A. acuta* has previously been the object of studies involving its great capability to specifically accumulate Ag (Genta-Jouve et al. 2012). The affinity of this sponge for Ag is probably associated to its metabolism. The present study proves that Ag in the form of NPs is also highly accumulated in these organisms. This aspect certainly deserves further study to better understand the Ag accumulation cycle, as well as the potential of sponges as bio-remediation organisms also for nanoparticle related pollution.

The present work provides a fast and fit-for-purpose method for the distinction and detection of Ag^+ and Ag NPs by SS-CS-HR-AAS in different marine biological matrices. The developed method was successfully applied to solid CRMs (mussel and fish homogenate) spiked with Ag^+ and Ag NPs solutions, and in all cases, it was possible to easily distinguish between the peaks obtained for the two Ag forms. Exposure experiments on living organisms (mussels and sponges) were also carried out, and the obtained results were very promising, demonstrating that the method can be successfully utilized to distinguish Ag^+ from Ag NPs in a variety of different organisms. Sponges, which had never been used for accumulation studies of Ag NPs, proved to be particularly promising biological tool for the bioremediation of marine areas contaminated with Ag NPs.

Acknowledgements The authors are grateful to Mr Angus Taylor and Mr François Oberhaensli for their assistance during exposure experiments with mussels and sponges. The agency is grateful for the support provided to its Marine Environment Laboratories by the Government of the Principality of Monaco.

Author contribution All authors contributed to the study conception and design. Material preparation and analysis were performed by AMO under the supervision of EV. The first draft of the manuscript was written by AMO. EV and OT reviewed and corrected it. All authors read and approved the final manuscript before submission.

Funding The authors declare that no funds, grants, or other support were received during the preparation of this manuscript.

Declarations

Competing interests The authors have no relevant financial or non-financial interests to disclose.

References

Abbott Chalew TE, Galloway JF, Graczyk TK (2012) Pilot study on effects of nanoparticle exposure on Crassostrea virginica hemocyte phagocytosis. Mar Pollut Bull 64:2251–2253. https://doi.org/10.1016/j.marpolbul.2012.06.026

Adamek D, Sliwinski J, Ostaszewska T et al (2018) Effect of Copper and Silver Nanoparticles on Trunk Muscles in Rainbow Trout (Oncorhynchus mykiss, Walbaum, 1792). Turkish J Fish Aquat Sci 18:781–788. https://doi.org/10.4194/1303-2712-v18_6_04

Artiaga G, Ramos K, Ramos L et al (2015) Migration and characterisation of nanosilver from food containers by AF4-ICP-MS. Food Chem 166:76–85. https://doi.org/10.1016/j.foodchem.2014.05.139

Batista D, Pascoal C, Cássio F (2020) The Increase in Temperature Overwhelms Silver Nanoparticle Effects on the Aquatic

Invertebrate Limnephilus sp. Environ Toxicol Chem 39:1429–1437. https://doi.org/10.1002/etc.4738
Blasco C, Picó Y (2011) Determining nanomaterials in food. TrAC Trends Anal Chem 30:84–99. https://doi.org/10.1016/j.trac.2010.08.010
Echegoyen Y, Nerín C (2013) Nanoparticle release from nano-silver antimicrobial food containers. Food Chem Toxicol 62:16–22. https://doi.org/10.1016/j.fct.2013.08.014
Fabrega J, Luoma SN, Tyler CR et al (2011) Silver nanoparticles: Behaviour and effects in the aquatic environment. Environ Int 37:517–531. https://doi.org/10.1016/j.envint.2010.10.012
Feichtmeier NS, Leopold K (2014) Detection of silver nanoparticles in parsley by solid sampling high-resolution – continuum source atomic absorption spectrometry. 3887–3894
https://doi.org/10.1007/s00216-013-7510-0
Feichtmeier NS, Ruchter N, Zimmermann S et al (2016) A direct solid sampling analysis method for the detection of silver nanoparticles in biological matrices. Anal Bioanal Chem 408:295–305. https://doi.org/10.1007/s00216-015-9108-1
Gagné F, Turcotte P, Gagnon C (2012) Screening test of silver nanoparticles in biological samples by graphite furnace-atomic absorption spectrometry. 404:2067–2072. https://doi.org/10.1007/s00216-012-6258-2
Genta-Jouve G, Cachet N, Oberhänsli F et al (2012) Comparative bioaccumulation kinetics of trace elements in Mediterranean marine sponges. Chemosphere 89:340–349. https://doi.org/10.1016/j.chemosphere.2012.04.052
Gomes T, Araújo O, Pereira R et al (2013) Genotoxicity of copper oxide and silver nanoparticles in the mussel Mytilus galloprovincialis. Mar Environ Res 84:51–59. https://doi.org/10.1016/j.marenvres.2012.11.009
Gruszka J, Martyna A, Godlewska-Żyłkiewicz B (2021) Chemometric approach to discrimination and determination of binary mixtures of silver ions and nanoparticles in consumer products by graphite furnace atomic absorption spectrometry. Talanta 230. https://doi.org/10.1016/j.talanta.2021.122319
Gruszka J, Zambrzycka-Szelewa E, Kulpa JS, Godlewska-Zyłkiewicz B (2018) Discrimination between ionic silver and silver nanoparticles in consumer products using graphite furnace atomic absorption spectrometry. J Anal At Spectrom 33:2133–2142. https://doi.org/10.1039/c8ja00310f
Handy RD, Henry TB, Scown TM et al (2008a) Manufactured nanoparticles: their uptake and effects on fish-a mechanistic analysis. Ecotoxicology 17:396–409. https://doi.org/10.1007/s10646-008-0205-1
Handy RD, Owen R, Valsami-Jones E (2008b) The ecotoxicology of nanoparticles and nanomaterials: current status, knowledge gaps, challenges, and future needs. Ecotoxicology 17:315–325. https://doi.org/10.1007/s10646-008-0206-0
Jokar M, Rahman RA (2014) Study of silver ion migration from melt-blended and layered-deposited silver polyethylene nanocomposite into food simulants and apple juice. Food Addit Contam Part A 31:734–742. https://doi.org/10.1080/19440049.2013.878812
Lee S, Bi X, Reed RB et al (2014) Nanoparticle Size Detection Limits by Single Particle ICP-MS for 40 Elements. Environ Sci Technol 48:10291–10300. https://doi.org/10.1021/es502422v
Leopold K, Brandt A, Tarren H (2017) Sizing gold nanoparticles using graphite furnace atomic absorption spectrometry. J Anal At Spectrom 32:723–730. https://doi.org/10.1039/c7ja00019g
Loeschner K, Navratilova J, Købler C et al (2013) Detection and characterization of silver nanoparticles in chicken meat by asymmetric flow field flow fractionation with detection by conventional or single particle ICP-MS. Anal Bioanal Chem 405:8185–8195. https://doi.org/10.1007/s00216-013-7228-z
Magesky A, Pelletier É (2018) Cytotoxicity and physiological effects of silver nanoparticles on marine invertebrates. Adv Exp Med Biol 1048:285–309. https://doi.org/10.1007/978-3-319-72041-8_17
Magesky A, Ribeiro CAO, Pelletier É (2016) Physiological effects and cellular responses of metamorphic larvae and juveniles of sea urchin exposed to ionic and nanoparticulate silver. Aquat Toxicol 174:208–227. https://doi.org/10.1016/j.aquatox.2016.02.018
Marambio-Jones C, Hoek EMV (2010) A review of the antibacterial effects of silver nanomaterials and potential implications for human health and the environment. J Nanoparticle Res 12:1531–1551. https://doi.org/10.1007/s11051-010-9900-y
McCarthy MP, Carroll DL, Ringwood AH (2013) Tissue specific responses of oysters, Crassostrea virginica, to silver nanoparticles. Aquat Toxicol 138–139:123–128. https://doi.org/10.1016/j.aquatox.2013.04.015
Navratilova J, Praetorius A, Gondikas A et al (2015) Detection of engineered copper nanoparticles in soil using single particle ICP-MS. Int J Environ Res Public Health 12:15756–15768. https://doi.org/10.3390/ijerph121215020
Ntim SA, Thomas TA, Begley TH, Noonan GO (2015) Characterisation and potential migration of silver nanoparticles from commercially available polymeric food contact materials. Food Addit Contam Part A 32:1003–1011. https://doi.org/10.1080/19440049.2015.1029994
Peters R, Herrera-Rivera Z, Undas A et al (2015) Single particle ICP-MS combined with a data evaluation tool as a routine technique for the analysis of nanoparticles in complex matrices. J Anal At Spectrom 30:1274–1285. https://doi.org/10.1039/c4ja00357h
Resano M, Garcia-Ruiz E, Garde R (2016) High-resolution continuum source graphite furnace atomic absorption spectrometry for the monitoring of Au nanoparticles. J Anal At Spectrom 31:2233–2241. https://doi.org/10.1039/c6ja00280c
Resano M, Mozas E, Crespo C et al (2010) Solid sampling high-resolution continuum source graphite furnace atomic absorption spectrometry to monitor the biodistribution of gold nanoparticles in mice tissue after intravenous administration. J Anal At Spectrom 25:1864–1873. https://doi.org/10.1039/c0ja00086h
Shaw BJ, Handy RD (2011) Physiological effects of nanoparticles on fish: A comparison of nanometals versus metal ions. Environ Int 37:1083–1097. https://doi.org/10.1016/j.envint.2011.03.009
Silva BF, Pérez S, Gardinalli P et al (2011) Analytical chemistry of metallic nanoparticles in natural environments. TrAC Trends Anal Chem 30:528–540. https://doi.org/10.1016/j.trac.2011.01.008
Tiede K, Boxall ABA, Tiede D et al (2009) A robust size-characterisation methodology for studying nanoparticle behaviour in 'real' environmental samples, using hydrodynamic chromatography coupled to ICP-MS. J Anal At Spectrom 24:964–972. https://doi.org/10.1039/B822409A
von Goetz N, Fabricius L, Glaus R et al (2013) Migration of silver from commercial plastic food containers and implications for consumer exposure assessment. Food Addit Contam Part A 30:612–620. https://doi.org/10.1080/19440049.2012.762693
Zhang W, Xiao B, Fang T (2018) Chemical transformation of silver nanoparticles in aquatic environments: Mechanism, morphology and toxicity. Chemosphere 191:324–334. https://doi.org/10.1016/j.chemosphere.2017.10.016